Development of Local Meteorological Model based on CFD Model

Ryosaku Ikeda[a], Hiroyuki Kusaka[a], Satoru Iizuka[b], Taisuke Boku[a]

[a]*University of Tsukuba, 1-1-1 Tennoudai Tsukuba, Japan*
[b]*Nagoya University, Furo-chou Chikusa-ku Nagoya, Japan*

ABSTRACT: We have been developed local meteorological model based on LES model. One of the methods of describing topography is by using standard terrain following coordinate system. However, the terrain following coordinate system poses a problem that the truncation error increases with a slope angle of more than 45º. In this study, we developed a LES model with generalized curvilinear coordinate system to overcome this problem. Several model verification tests are performed to evaluate the accuracy of the dynamics, physics, coordinate transformation, and the effects of stratification. From these results it can be concluded that at present, our model is correctly developed, at least with regarding the dynamics, physics, boundary conditions, and coordinate transformation. For further verification, numerical tests over steep slope mountains were performed. It is shown that models using the z* coordinates simulates results with computational error over steep slope mountains, but remarkable numerical error was not found with the generalized curvilinear coordinate system even when the slope angle is 59.0º. Finally, parallel computation tests are performed on the super computer, T2K-Tsukuba. As a result, the parallelization efficiency is confirmed to be about 0.5 when 1024 processors are used.

KEYWORDS: Large eddy simulation, Generalized curvilinear coordinate system, Steep slope terrain, Parallel computation

1 INTRODUCTION

Large eddy simulation (LES) is a numerical modeling approach which explicitly calculates the large eddy field and parameterizes the small eddies. In the meteorological field, this approach has been used to examine detailed turbulence structure, perform physical process studies, and to develop a parameterization scheme for ensemble mean turbulent models. Until today, most LES applications for meteorological studies have been limited to idealized physical conditions (e.g. horizontally uniform surfaces). There are several methods of describing topography in atmospheric models; cartesian coordinate system (e.g. Raasch and Schroter 2001), terrain following coordinate system (e.g. Chow et al. 2006), and Immersed Boundary Method (e.g. Fadlum et al. 2000). However, the terrain following coordinate system causes problems as the truncation error increases with a slope angle of more than 45º. In this study, we develop a LES model with generalized curvilinear coordinate system to overcome this problem.
LES models are known for their large demands of computer resources; so the parallelization was performed using MPI in our model.

2 MODEL DESCRIPTION

2.1 *Atmospheric model*

In this section, we briefly describe the LES model developed in this study. This model is based on the CFD model developed by Satoru Iizuka (associate professor at Nagoya University). The governing equations utilized for the basic variables, after application of space filtering and coordinate transformation are:

$$\frac{\partial \overline{U}_m}{\partial \xi_m} = 0$$

$$\frac{\partial \overline{u_i}}{\partial t} + \frac{1}{J}\frac{\partial \overline{U}_m \overline{u_i}}{\partial \xi_m} = -\frac{1}{J}\frac{\partial}{\partial \xi_m}\left(J\frac{\partial \xi_m}{\partial z}(c_p\theta_0\overline{\Pi'})\right) + \frac{1}{J}\frac{\partial}{\partial \xi_m}\left[J\frac{\partial \xi_m}{\partial x_j}\left\{-\tau_{ij} + \nu\frac{1}{J}\frac{\partial}{\partial \xi_n}\left(J\frac{\partial \xi_n}{\partial x_j}\overline{u_i}\right)\right\}\right] + F_i$$

$$\frac{\partial \overline{\theta'}}{\partial t} + \frac{1}{J}\frac{\partial \overline{U}_m \overline{\theta}}{\partial \xi_m} = \frac{1}{J}\frac{\partial}{\partial \xi_m}\left[J\frac{\partial \xi_m}{\partial x_j}\left\{-\tau_{\theta j} + \kappa\frac{1}{J}\frac{\partial}{\partial \xi_n}\left(J\frac{\partial \xi_n}{\partial x_j}\overline{\theta'}\right)\right\}\right]$$

where u_i is the ith velocity component (i, j run from 1 to 3), U_i is the contravariant velocity component, Π is the exner function, θ is potential temperature, τ_{ij} is the subgrid stress tensor, $\tau_{\theta j}$ is the subgrid turbulent flux for heat. The overbar refers to a resolved-scale variable. The Boussinesq approximation has been applied here, and θ_0 is the constant repressentative value of potential temperature. The subgrid tensor and subgrid turbulent flux have to be modelled to close the basic equations. Our model adopted the Smagorinsky model and Deardorff's model (Deardorff 1980). Numerical schemes are listed in Table 1.

Table 1. Model description.

Basic equations	Boussinesq approximation
Coordinate	General curvilinear coordinate system
Discretization approach	Finite difference method
Grid System	Colocation
Time integration scheme	
Advection term	2nd order Adams-Bashforth method
Diffusion term	Crank-Nicolson scheme
Spatial difference	2nd order central
Solution method for the equations	SMAC
Solution method for the poisson equation	Bi-CGStab method
Turbulence	LES (Smagorinsky, Deardorff(1980))

3 VERIFICATION TESTS

Several model verification tests are performed to evaluate the accuracy of the dynamics, physics, boundary conditions, coordinate transformation, and the effects of stratification.

3.1 *Verification tests*

Firstly, we conducted the idealized simulations of the wind, temperature, and turbulent fluxes within two types of planetary boundary layers (PBL); a shear-driven PBL flow (Case A) and a buoyancy dominated flow (Case B). The results show a streaky structure apparent in the shear-driven PBL flow, whereas this structure is absent in the buoyancy dominated flow (Fig.1). For the buoyancy dominated flow, the height of the mixed layer is in good agreement with the theoretical PBL flow (Figure is omitted). Figure 2a and 2b show the turbulent heat flux and energy (Case B), respectively. As expected, the SGS effect is very small except for near the surface. Furthermore, the TKE budgets are in good agreement with theory and earlier studies for both cases. In Case A, the shear production term nearly balances the dissipation term within the PBL. In Case B, the primary source term is buoyancy, while the shear production term has a large value only near the surface and the dissipation term is nearly uniform in the mid- to upper boundary layer (Figure is omitted).

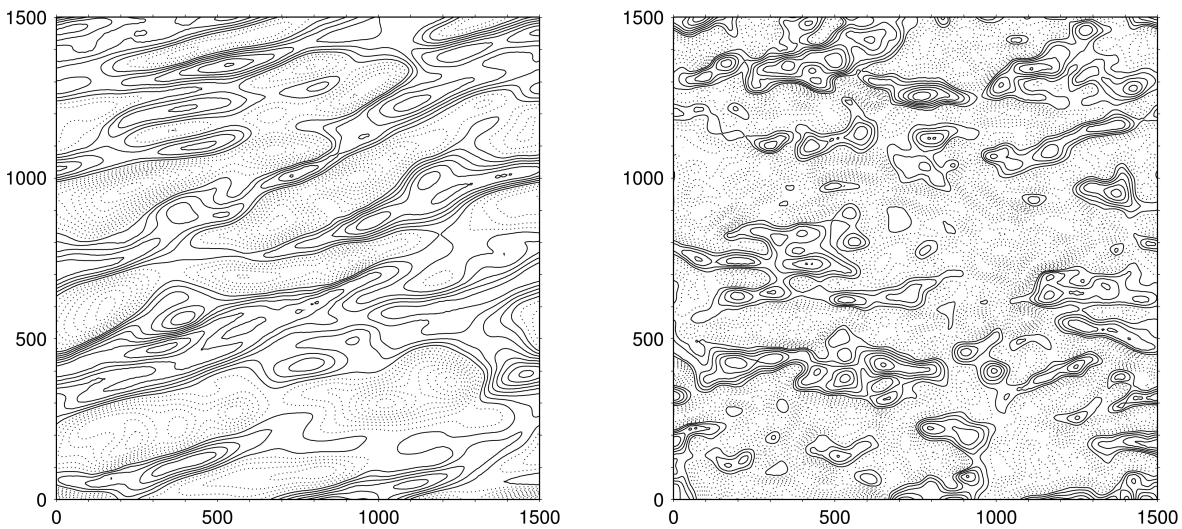

Figure 1. Contours of flow variables in the x-y plane at $z/z_i = 0.1$ for Case A (left figure) and Case B (right figure), respectively.

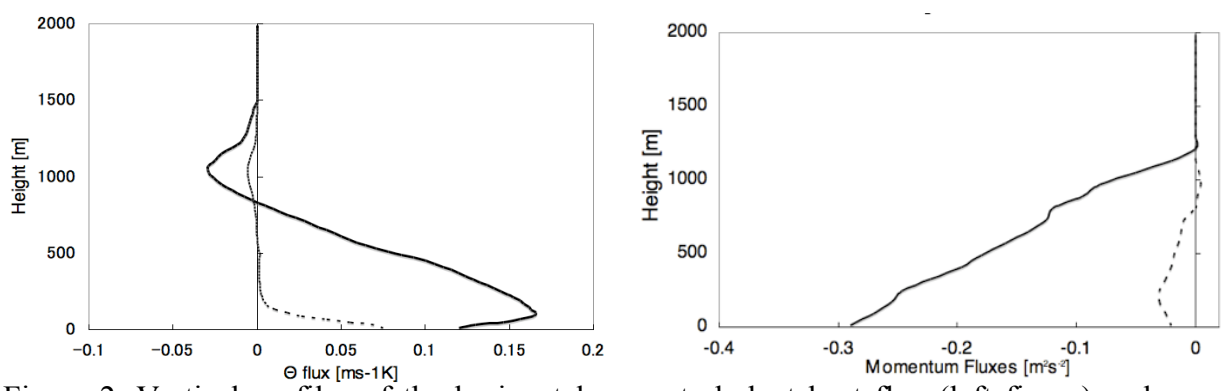

Figure 2. Vertical profiles of the horizontal mean turbulent heat flux (left figure) and energy (right figure) of the resolvable field (solid line) and the subgrid-scale field (dashed line), respectively.

Secondly, numerical simulations of mountain waves under the idealized conditions were carried out. We performed three types of mountain wave calculations; damped waves, vertically propa-

gating waves, and leeward propagating waves. The simulated results indicate that the propagating direction, wave pattern, and momentum fluxes are in good agreement with the theoretical solutions (Figure is omitted).

From these results, it can be concluded that at present, our model is correctly developed at least with regarding the dynamics, physics, and coordinate transformation.

3.2 *Numerical simulation against steep slope terrain*

As the horizontal resolutions of atmospheric numerical model are increasing, steep slopes are resolved in models. To examine the accuracy of the generalized curvilinear coordinate system, some numerical tests under steep slope terrain were performed. For a bell-shaped mountain, the height of the mountain is 100m, and is set at the center of the domain. Simulations were performed for three types of mountains with a half width of 50m, 40m, and 30m. The averaged mountain slope angles are 45.0º, 51.3º, and 59.0º, respectively. The Brant-Väisäla frequency is 0.02, the Scorer parameter is 0.002, the height of the model top is 2km, and the integration time is 5min. Numerical tests also performed for the z* coordinate under the same conditions.
The results for the 45.0º slope angle did not show remarkable numerical errors, even in the z* coordinate system. However, when the slope angle is 51.3º, numerical error appeared in the z* coordinate system. As the slope angle reached 59.0º, the numerical error increased. Remarkable numerical error was not found for the generalized curvilinear coordinate system even when the slope angle is 59.0º.

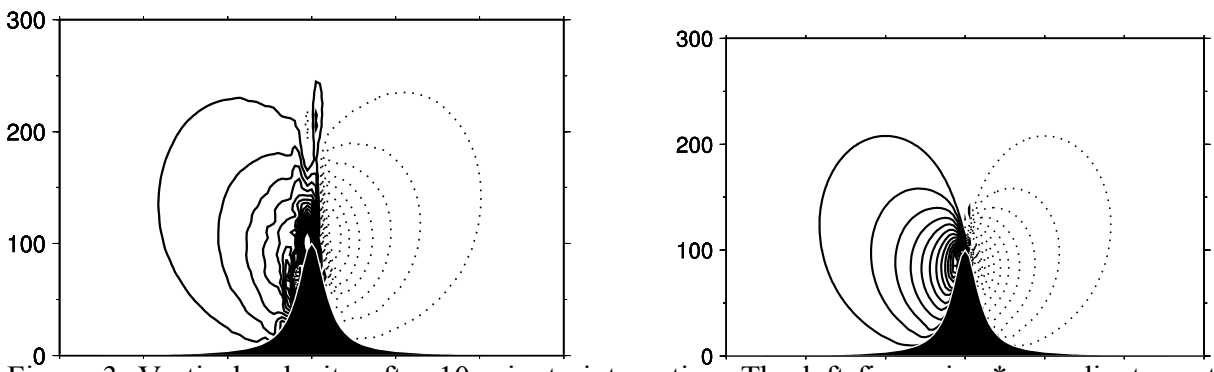

Figure 3. Vertical velocity after 10 minute integration. The left figure is z* coordinate system and the right figure is generalized curvilinear coordinate system.

4 PARALLELIZATION

The numerical model was tested on the T2K-Tsukuba system. The machine consists of 648 compute nodes providing 95.4 Tflops of computing capability. Each node consists of quad-socket, 2.3 GHz Quad-Core AMD Opteron Model 8356 processors whose on-chip cache sizes are 64 KBytes/core, 512 KBytes/core, 2 MB/chip for L1, L2, L3, respectively. Each processor has a direct connect memory interface to an 8 GBytes DDR2-667 memory and three hypertransport links to connect other processors. All the nodes in the system are connected through a full-bisectional fat-tree network consisting of four interconnection links of 8 GBytes/sec/direction aggregate bandwidth with Infiniband 4xDDR.
In the parallelization, MPI was used to transfer information between the processors.

4.1 *Fixed-domain test*

A fixed-domain test is the number of grid points in the domain which is kept constant as the processors are added. For this test, as the number of processor is increased, each processor has fewer gird points.

A convective boundary layer was used for this test. The domain has 320x320x100 grid points. The results are presented in Fig. 5, where "speedup" is the ratio of time required to run the simulation on one processor, to the time required to run *n* processors. For perfect parallelization, the speedup would be identical to the number of processors used. In our model, the results are nearly perfect out of the 128 processors.

The Parallel efficiency is provided below:

$$\text{Parallel efficiency} = 100 \times \frac{speedup}{n}.$$

Ideally, a parallel efficiency of 100% is desired. The results of the test show that parallel efficiency is over 80% under 128 processors, and drops to about 45% with 1024 processors.

For further study, scaled-domain tests will be carried out in the future.

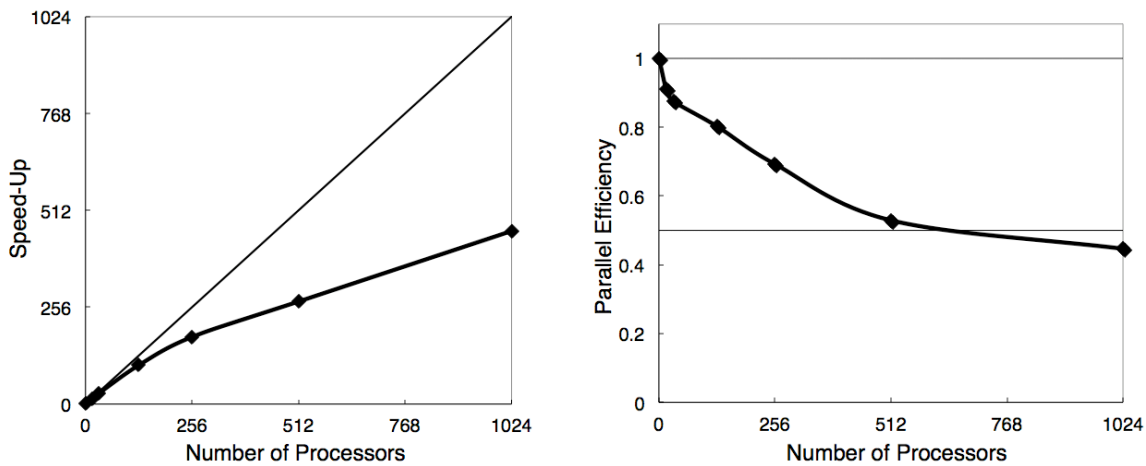

Figure 4. Parallel performance for the fixed-domain test: (a) speedup versus number of processors; and (b) parallel efficiency.

5 CONCLUSIONS

We developed a local meteorological model based on the LES model. Several verification tests were performed. From these numerical test results, it can be concluded that at present, our model is correctly developed at least with regarding the dynamics, physics, and coordinate transformation. For further verification, numerical tests over steep slope mountains were performed. It is shown that models using the z* coordinates simulates results with computational error over steep slope mountains, but with the generalized curvilinear coordinate system, remarkable numerical error was not found even when the slope angle is 59.0º. Finally, parallel computation tests are performed on the super computer, T2K-Tsukuba. The results show that parallel efficiency is over 80% under 128 processors, and drops to about 45% with 1024 processors.

Acknowledgements

The present study was supported by the Research Program on Climate Change Adaptation (RECCA). This work was supported by the "Interdisciplinary Computational Science Program" in the Center for Computational Sciences, University of Tsukuba.